

This item is the archived peer-reviewed author-version of:

The influence of plant species, leaf morphology, height and season on PM capture efficiency in living wall systems

Reference:

Koch Kyra, Wuyts Karen, Denys Siegfried, Samson Roeland.- The influence of plant species, leaf morphology, height and season on PM capture efficiency in living wall systems
The science of the total environment - ISSN 1879-1026 - 905(2023), 167808
Full text (Publisher's DOI): <https://doi.org/10.1016/J.SCITOTENV.2023.167808>
To cite this reference: <https://hdl.handle.net/10067/2010330151162165141>

1 The influence of plant species, leaf morphology, height and season on PM
2 capture efficiency in living wall systems

3

4 Abstract

5 Green infrastructure (GI) is already known to be a suitable way to enhance air quality in urban
6 environments. Living wall systems (LWS) can be implemented in locations where other forms of GI, such
7 as trees or hedges, are not suitable. However, much debate remains about the variables that influence
8 their particulate matter (PM) accumulation efficiency. This study attempts to clarify which plant species
9 are relatively the most efficient in capturing PM and which traits are decisive when it comes to the
10 implementation of a LWS. We investigated 11 plant species commonly used on living walls, located close
11 to train tracks and roads. PM accumulation on leaves was quantified by magnetic analysis (*Saturation*
12 *Isothermal Remanent Magnetization* (SIRM)). Several leaf morphological variables that could potentially
13 influence PM capture were assessed, as well as the Wall Leaf Area Index. A wide range in SIRM values (2.74
14 - 417 μA) was found between all species. Differences in SIRM could be attributed to one of the
15 morphological parameters, namely SLA (specific leaf area). This suggest that by just assessing SLA, one can
16 estimate the PM capture efficiency of a plant species, which is extremely interesting for urban greeners.
17 Regarding temporal variation, some species accumulated PM over the growing season, while others
18 actually decreased in PM levels. This decrease can be attributed to rapid leaf expansion and variations in
19 meteorology. Correct assessment of leaf age is important here; we suggest individual labeling of leaves for
20 further studies. Highest SIRM values were found close to ground level. This suggests that, when traffic is
21 the main pollution source, it is most effective when LWS are applied at ground level. We conclude that

22 LWS can act as local sinks for PM, provided that species are selected correctly and systems are applied
23 according to the state of the art.

24

25 1 Introduction

26 Particulate matter (PM) pollution is one of the major challenges in urban environments nowadays. Even
27 though PM_{2.5} concentrations in urban environments decreased by approximately 20% between 2005 and
28 2015, EU air quality standards have not been met (EEA, 2017a; EEA, 2017b). Epidemiological studies show
29 a strong correlation between PM pollution and adverse health effects (Pope III and Dockery 2006; Solomon
30 et al. 2012; Van Dyck et al. 2019). Besides severe health effects and premature mortality (Brunekreef
31 1997), PM pollution also causes damage to the environment, crops and infrastructure (Jimoda et al. 2012;
32 Rai et al. 2016).

33 Urban green infrastructure (UGI) such as trees, hedgerows, green roofs and green walls can act as a natural
34 filter for PM and contribute to air pollution mitigation by deposition of particles on plant leaves (Beckett,
35 Freer-Smith, and Taylor 1998; Litschke and Kuttler 2008; Nowak, Crane, and Stevens 2006; Pugh et al.
36 2012; Shao et al. 2021). Deposition effects related to vegetation were studied by Gallagher et al. (2015)
37 and Janhäll (2015), among others. Moreover, Abhijith et al. (2017) discussed the comparison of different
38 UGIs on air quality improvement. However, due to the *street canyon* effect, models suggest that trees can
39 sometimes have a negative impact on local air quality (Vos et al. 2012) by hampering air flow. In contrast,
40 green walls (vertical structures covered by vegetation) do not inhibit free air flow through the street
41 canyon and thus can also have a positive impact on urban air quality, when applied appropriately.
42 Moreover, green walls provide many more ecosystem services than PM mitigation, such as cooling the
43 ambient air and underlying walls (Pérez et al. 2011; Wong et al. 2010; Koch et al. 2020), increasing
44 biodiversity (Madre et al. 2015), water retention and purification (Prodanovic et al. 2017; van de Wouw et

45 al. 2017; Hussain Lakho et al. 2021), carbon sequestration (Tallis et al. 2015) and social and cultural benefits
46 (White and Gatersleben 2011).

47 Recently, some interesting studies have been published regarding green walls and their potential to
48 capture PM, on which a review was published by Ysebaert et al. (2021). Literature mainly considered soil-
49 bound Ivy (*Hedera helix*) (Ottel  et al. 2010; Sternberg et al. 2010; Przybysz et al. 2014), although (Perini
50 et al. 2017) studied several other climber plant species and (Weerakkody et al. 2017, 2018a, 2018b and
51 Viecco et al. 2018) reported about living wall systems (LWS). LWS are systems in which plants that normally
52 grow in the soil are rooted in a substrate material, directly attached to the wall (Koch et al. 2020). The
53 substrate can be pre-cultivated panels, bags, textiles or other materials, and can be of natural composition
54 (soil, moss) or synthetic. There is always an irrigation system that also includes nutrient distribution over
55 the plants. This kind of system facilitates the use of a wide variety of plant species, from small herbs to
56 medium sized shrubs.

57 Plant species, all of which have their own unique morphological and physiological characteristics, are
58 typically characterized by different PM capture qualities according to this review paper. The importance
59 of selecting plants with certain traits is also highlighted by Litschke and Kuttler (2008), Weerakkody et al.
60 (2017), Muhammad et al. (2019) and others. It was found that plant leaves with a higher wax content
61 (Perini et al. 2017), higher wettability (Muhammad et al. 2019; Wang et al. 2013) or with a higher stomatal
62 density (Weerakkody et al. 2018b) collect more particles. The influence of trichomes is still considered
63 inconclusive for green wall studies. Hairy leaves were less effective in PM capture according to Perini et al.
64 (2017) while hairiness was considered insignificant according to Weerakkody et al. 2018b). This is in
65 contrast to other studies on more than hundred tree, shrub and climber species (S eb  et al. 2012; Kardel
66 et al. 2012; Muhammad et al. 2019) and herbaceous plants (Weber et al; 2014), which report important
67 differences between hairy and non-hairy leaves and significant positive relationships between PM

68 accumulation and trichome density. To summarize, we assume that the amount of LWS species considered
69 is too small to make decent comparisons with the large amount of tree species considered in literature.

70 Leaf shape was also considered an important variable, with small and needle-like leaves being better PM
71 accumulators (Beckett et al. 2000; Dzierzanowski et al. 2011). The specific leaf area (SLA, the amount of
72 one-sided leaf surface divided by its dry mass) appears to be a good predictor of PM accumulation and
73 immobilisation for trees, as a proxy for the complex interactions of various leaf morphological
74 characteristics (Muhammad 2019, 2020). In contrast, a recent study conducted by Paull et al. (2019) on
75 11 common green wall plant species found minimal evidence for the influence of leaf morphology on PM
76 accumulation, but nevertheless reported differences between species.

77 Pollution level is another important factor to be considered. Several studies suggest that the load of
78 captured particles on the leaves is higher when the pollution level is higher (Ottelé et al. 2010; Sternberg
79 et al. 2010; Kardel et al. 2012; Przybysz et al. 2014). In our study, however, pollution level is constant due
80 to the nature of the experimental setup; a common garden with similar outdoor conditions and sources,
81 which implies that differences between species can be attributed to other parameters. Also wind speed,
82 turbulence, relative air humidity and precipitation can influence particle deposition and accumulation on
83 plants (Litschke and Kuttler 2008; Weerakkody, John W Dover, et al. 2018).

84 For living wall systems (LWS) in particular, insufficient research has been conducted in terms of their PM
85 mitigation capacity, and the few studies conducted have produced inconsistent results concerning
86 relevant parameters. Furthermore, the effects of height on PM deposition are generally poorly understood
87 due to the lack of studies. However, green walls offer the opportunity to capture PM at lower heights than
88 urban trees, e.g. they can be applied at pedestrian height, while tree canopies are situated higher above
89 the ground. Furthermore, the seasonal dynamics and height variation of PM accumulation on leaves in
90 LWS were studied.

91 In this study, it is examined to which extent PM accumulation on plants in LWS is determined by plant
92 species and their leaf characteristics, utilizing biomagnetic analysis (SIRM; *Saturation Isothermal*
93 *Remanent Magnetization*) (Hofman et al. 2013; Matzka and Maher 1999). We aim to provide suggestions
94 to optimize the design of living wall systems in terms of plant species selection to maximise PM mitigation.
95 Moreover, the influence planting height on PM load and seasonal variation within these plant species are
96 included in the analysis. We hypothesize that smaller, hairier leaves with lower SLA and at lower height
97 perform better in terms of PM accumulation capacity. Furthermore we expect an increase in PM load on
98 the plants over the growing season.

99

100 2 Materials & methods

101 2.1 Test location

102 Plant samples were collected at the Testing Center for Floriculture (Proefcentrum voor Sierteelt, hereafter
103 referred to as PCS) in Destelbergen, Belgium (lat. = 51.071744° N, lon. = 3.812062° E) (Appendix Figure 1).
104 This site has a large amount of LWS which are all exposed to the same external conditions. Local pollution
105 sources originated from the background concentrations of the city of Ghent, the Port of Ghent and the
106 steel manufacturer Arcelor-Mittal, located west of the test site. The impact of the Arcelor-Mittal
107 metallurgic factory on airborne pollution was discussed by (Declercq et al. 2020) Considering the main
108 southwest wind direction in Belgium, the test site is located more or less downwind of these urban sources.
109 Furthermore, a calm street and a railroad are located in close proximity of the test site; approximately 10
110 m westward and 100 m northward, respectively. The busy ring road R4 is located approximately 400 m
111 west of the test area.

112

113 2.2 Sample collection

114 The test facility contains 13 southwest-facing living wall systems (LWS, wall-ID 1-13), constructed in 2016
115 and developed by different manufacturers from Belgium and the Netherlands (Appendix Figure 2). The
116 LWS contained a wide variety of plant species, an overview of which is given in Appendix table 1. A total
117 of 11 species were sampled and only species that were sufficiently present for sampling without visibly
118 damaging the system were selected for the experiment. However, not every plant species was present on
119 each testing wall and some testing walls (wall 1 to 5 and 11) were removed during the experiment
120 (Appendix table 2). Samples were collected in spring (28/04, sampling moment 1) and summer (24/08,
121 sampling moment 2) of 2017 and spring (20/03, sampling moment 3) of 2018.

122 Since individual plants had been present for a year at the time of first sampling, environmental pollution
123 level was equal for all systems (common garden) and the plants had developed fresh leaves since then, so
124 that differences in plant origin were considered negligible. For magnetic analysis, from each species 4 to
125 10 healthy leaves (depending on the availability and to have a sufficient leaf area for testing) were
126 collected at three different heights: (2.5 ± 0.2) m (A), (1.5 ± 0.2) m (B) and (0.5 ± 0.2) m (C). In order to
127 avoid contamination, the leaves were put into paper bags immediately after cutting and stored at 7°C for
128 up to maximum 48 hours before further analysis in the lab.

129

130 2.3 Meteorological conditions

131 Meteorological data for the entire sampling period and four extra months before were obtained from the
132 Flanders Environmental Agency (VMM) for the nearby station M701 at Tolhuiskaai, Gent. Appendix Figure
133 3 shows that temperatures never fell below -5°C and never rose above 27°C. According to Köppen Climate
134 Classification, our study area is situated in zone Cfb which is a temperate oceanic climate.

135

136 2.4 Leaf morphological variables

137 All leaf analyses were performed in the Laboratory of Environmental and Urban Ecology of the Bioscience
138 Engineering Department of the University of Antwerp, Belgium. For each species considered, a series of
139 leaf morphological variables was determined with the aim of determining key characteristics for PM
140 capture. This was done at one sampling moment, taking only mature leaves into account. A set of
141 morphological parameters were determined for 5 leaves per species (Appendix table 4) unless mentioned
142 otherwise.

143 The *drop contact angle* (DCA, degrees) describes the internal angle between the perimeter of a water
144 droplet and the leaf contact surface, and is a measure for the hydrophobicity of the leaf (Muhammad et
145 al. 2020). Leaves with a higher DCA have a higher hydrophobicity and are less wettable. To assess this
146 variable, ~~two~~ fresh leaves collected on the same day and treated within 6 hours of harvesting were used.
147 The studied leaf was cut in half and the two parts were fixed to a surface with either the adaxial or the
148 abaxial leaf side facing upwards using double-sided tape. A 7.5 μL droplet of distilled water was put on
149 both the adaxial and abaxial side of a leaf. A picture was taken with a Canon EOS 550D camera with a
150 macro lens (MP-E 65 mm 1:2.8) with 3 \times magnification. For image processing, the software ImageJ was
151 used with the plugin 'Low-Bond Axisymmetric Drop Shape Analysis' (LB-ADSA) (Stalder et al. 2010)(Stalder
152 et al. 2010) to determine the mean of the left and right drop contact angles. Some examples of different
153 DCA's are shown in Appendix Figure 4.

154 The *specific leaf area* (SLA, $\text{m}^2 \text{kg}^{-1}$) is the ratio between the one-sided fresh leaf area (A_{leaf}) and the leaf
155 dry mass (M_{leaf}). For this, 10 fresh leaves per plant species were scanned maximum 24 hours after sampling
156 with an HP Scanjet G3100 scanner and leaf area was measured in ImageJ. Dry mass of the leaves was
157 measured with an analytical balance (S-234, Denver Instruments, NY, USA, accuracy= 0.1 mg), after drying
158 for at least 160h at 40°C.

$$\text{Specific leaf area (SLA)} = \frac{A_{\text{leaf}}}{M_{\text{leaf}}}$$

159
160 The *leaf dissection index* (LDI, dimensionless)) describes leaf shape and is the ratio of the leaf
161 circumference (P_{leaf}) to the root of the leaf area ($\sqrt{A_{\text{leaf}}}$) (McLellan and Endler 1998). The lowest value is
162 3.545 which is for a circular leaf, while a high LDI means long or serrated leaf shape (Koch, Samson, and
163 Denys 2019). For species with compound leaves, LDI is taken for one leaflet only.

$$\text{Leaf dissection index (LDI)} = \frac{P_{\text{leaf}}}{\sqrt{A_{\text{leaf}}}}$$

164
165 The *functional leaf size* (FLS) is determined by dividing the largest circular area in the leaf (A_{circle}) by the
166 leaf area (A_{leaf}). This is a good measure for leaf boundary layer size, which is an important factor for PM
167 deposition (Koch et al. 2019, 2020). For species with compound leaves, FLS is taken for one leaflet instead
168 of the whole leaf as we assume this is aerodynamically more correct.

$$\text{Functional leaf size (FLS)} = \frac{A_{\text{circle}}}{A_{\text{leaf}}}$$

169
170 Finally, *hairiness* of leaves was determined by visual examination of the DCA images. Three classes were
171 determined: no visible hairs (0), visually short hairs (1) and visually long hairs (2) (Appendix Figure 4) as
172 viewed through the macro lens. This was based on the amount and the length of trichomes.

173
174 2.5 Magnetic analysis

175 PM accumulation on leaves was assessed using biomagnetic analysis as described by (Kardel et al. 2011,
176 2012; Hofman et al. 2014a, b). Hofman et al. (2017) published a review covering all knowledge upon the
177 publication date about PM deposition on biological surfaces. In this method, dried leaves were first tightly
178 wrapped in cling film and placed in small plastic containers of 10 cm³. Next, the leaf samples were

179 magnetized (*Molspin pulse magnetiser*) in a magnetic field of 800 mT and the remanent magnetisation (in
180 A/m) was measured in a *Molspin Minispin* magnetometer. In this way, the SIRM (*saturation isothermal*
181 *remanent magnetisation*) was determined by multiplying the volume of the container for the remanent
182 magnetization and normalizing for leaf area or mass. This variable is an indicator of atmospheric traffic-
183 and industry-related particulate matter and metals (Kardel et al. 2012; Maher et al. 2013). The SIRM values
184 were normalized both for mass (SIRMM, A . m² . kg⁻¹ . 10⁶), measured with a scientific balance (S-234,
185 Denver Instruments, NY, USA, accuracy= 0.1 mg) and for fresh leaf area (SIRMa, μA) which was determined
186 with a Li-3100 leaf area meter (Li-cor Inc., Lincoln, NE, USA). In total, 578 leaf samples were magnetically
187 analyzed.

188

189 2.6 Wall Leaf Area Index and upscaling

190 The *wall leaf area index* (WLAI) is a dimensionless number that describes the amount of one sided leaf
191 area compared to the amount of covered wall surface (Koch, et al. 2020; Ysebaert et al. 2021). Often the
192 *leaf area index* is used to describe tree canopy cover, but for vertical green elements, the leaf area index
193 has been expanded to the wall leaf area index. This is an important parameter, as it can be used to calculate
194 the total amount of PM capture per unit wall surface covered by LWS, and is calculated as:

$$195 \quad \text{WLAI} = \frac{\text{leaf surface (m}^2\text{)}}{\text{wall surface (m}^2\text{)}}$$

196 To assess this parameter, for every plant species a 50x50 cm square was cut out of one of the experimental
197 green walls. This was done during the pruning season in August. Leaf areas were determined for fresh
198 leaves.

199 SIRMa data provide information about how much magnetic particulate matter is accumulated on a certain
200 amount of leaf surface of a certain plant species (Hofman et al. 2014). But plant species themselves also

201 differ in how much leaf surface they actually have. Therefore, the SIRM was scaled up with WLAI to create
202 a variable called totalSIRM (total normalized SIRM), to give an idea of the total PM capture per unit of wall
203 surface area.

$$204 \quad \text{totalSIRM } (\mu A) = \text{SIRMa } (\mu A) \times \text{WLAI}$$

205

206 2.7 Statistical analysis

207 Data were analyzed in R version 3.3.1 (<https://cran.r-project.org/>). In this study, a difference is considered
208 significant if the p value is ≤ 0.05 . Because of non-normality according to a Shapiro-Wilk normality test,
209 the SIRM data were ln transformed. A mixed model (lme) was used to test SIRM values against species,
210 sampling time, height and wall-ID (as a random factor). Some LWS have been analyzed more often than
211 others and because some species have been measured multiple times on the same LWS. This means that
212 SIRM values of species from the same wall can be expected to be more similar than on different walls,
213 because they are in a slightly different location. In order to know the significant differences in SIRMm and
214 SIRMa values between species, the order of species names in the model was changed until all
215 combinations were made. The same was done for the variables sampling time and height. Differences
216 between sampling times per species for both SIRM analyses regarding seasonal variation were retrieved
217 with ANOVA. Furthermore, correlations of all morphological parameters were tested against each other.
218 Because the morphological parameters were not taken from the same leaves as the SIRMm and SIRMa
219 values, the average SIRM values per plant species were tested with a linear model against all leaf
220 morphological parameters. Values that were almost significant were isolated and retested against SIRM
221 parameters.

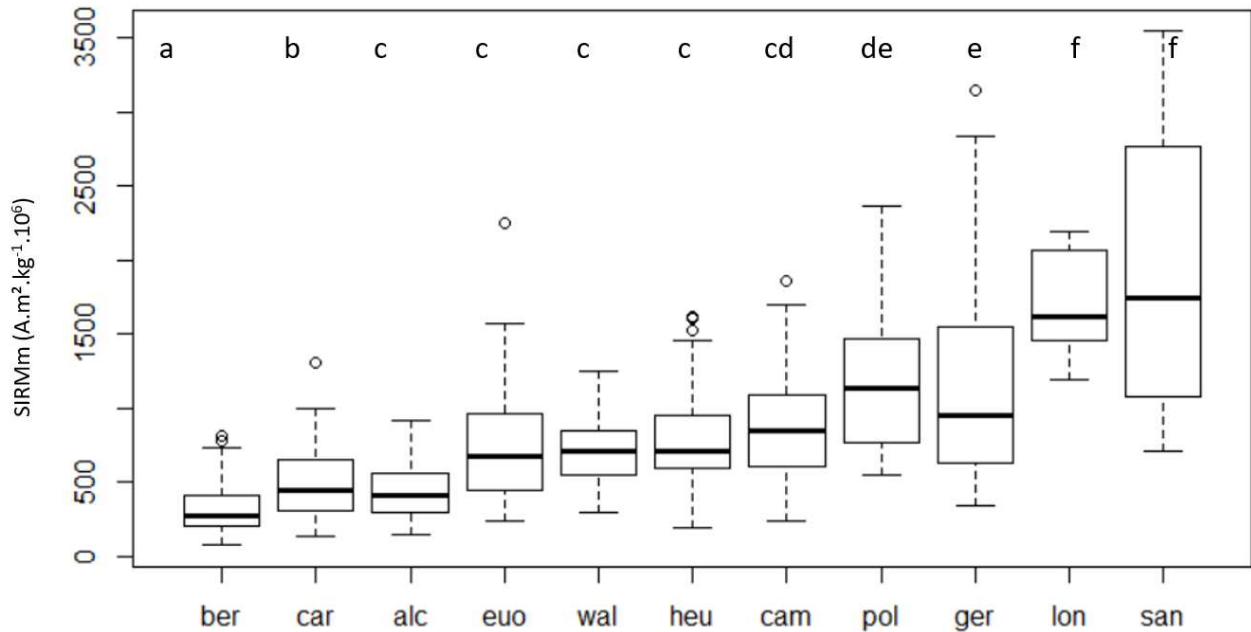
222

223 3 Results

224 3.1 Difference in PM accumulation between species

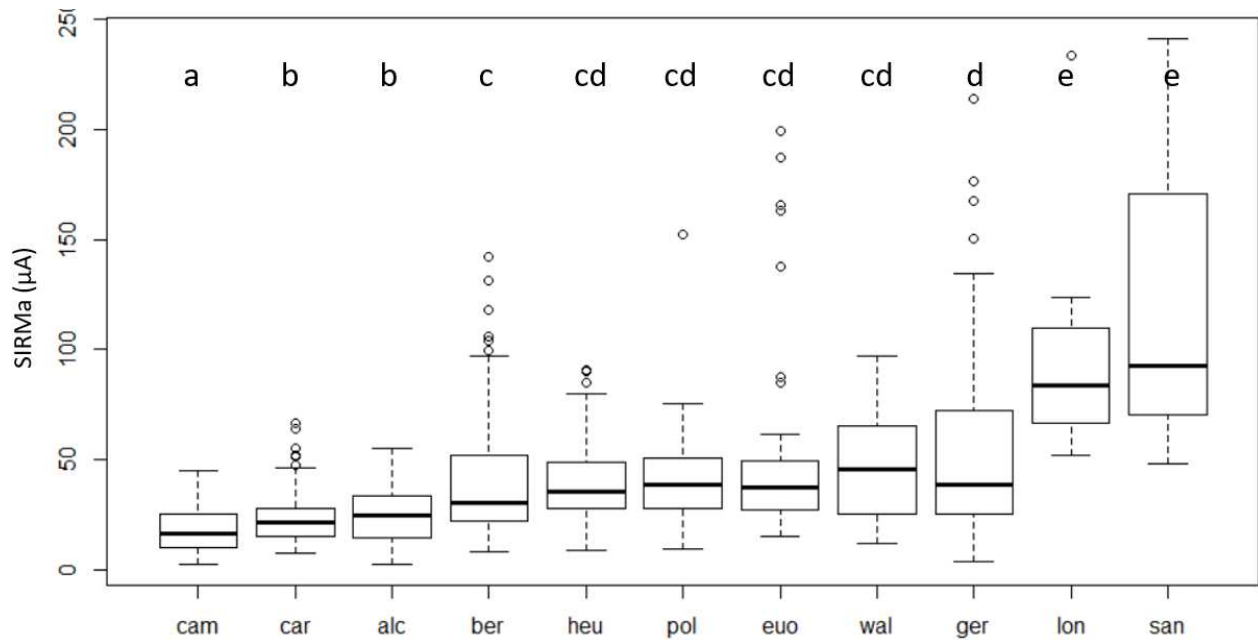
225 The SIRM values per species normalized for mass (SIRMm), averaged for all sampling moments and all
226 heights, ranged between 74.17 and 3543.22 $\mu\text{A m}^2 \text{kg}^{-1}$ and are plotted in ascending order of log values in
227 Figure 1. Figure 2 shows the surface area normalized SIRM (SIRMa) (values of 2.74 up to 417 μA). There
228 were significant differences in SIRM signal between species, of which *Bergenia cordifolia* scored lowest for
229 mass normalization while *Santolina chamaecyparissus* scored highest. *Santolina chamaecyparissus* also
230 scored highest for area normalization, but *Campanula* sp. scored the lowest.

231



232
233 Figure 1: Boxplot of the leaf dry mass normalized SIRMm-values for all species, with indication of the mean,
234 the first and third quartile, minimum and maximum values. Species abbreviations can be found in
235 Appendix table 1. Species with different letters (a-f) are significantly ($p < 0.05$) different.

236

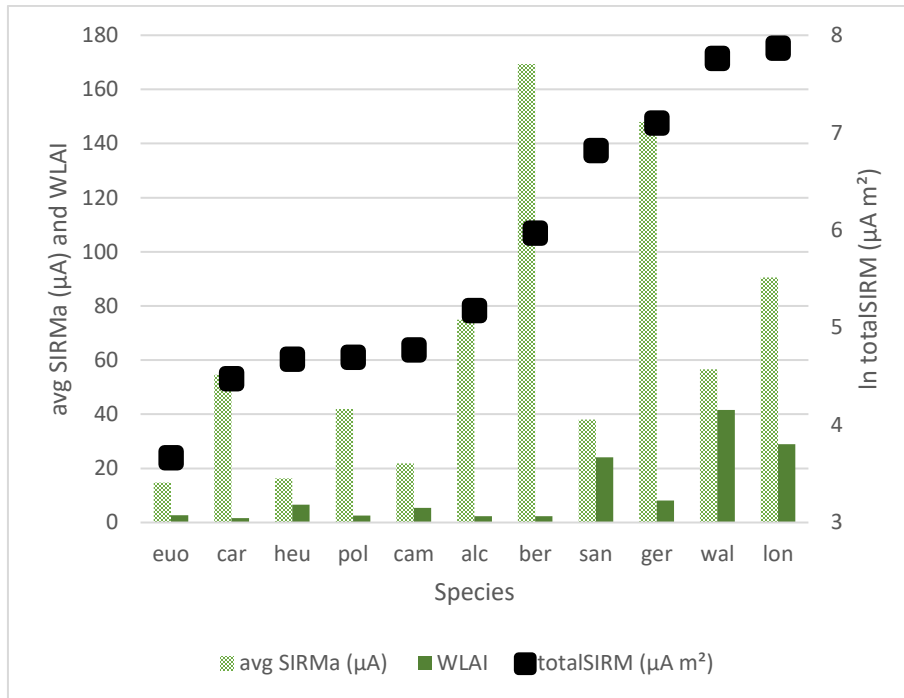


237
 238 Figure 2: Boxplot of the leaf area normalized SIRMa-values for all species, with indication of the mean, the
 239 first and third quartile, minimum and maximum values. Species abbreviations can be found in Appendix
 240 table 1. Species with different letters (a-e) are significantly ($p < 0.05$) different.

241

242 3.2 TotalSIRM: average SIRMa normalized for WLAI

243 As mentioned earlier, in order to understand how much PM can be captured by a certain amount of foliage,
 244 it is important to know how much leaf surface is available per unit of wall surface area. In order to obtain
 245 comparable numbers, only SIRMa values of the first sampling campaign were considered, as this was the
 246 sampling with the most samples of most species (see Appendix table 2). Figure 3 shows totalSIRM values
 247 of species in ascending order.



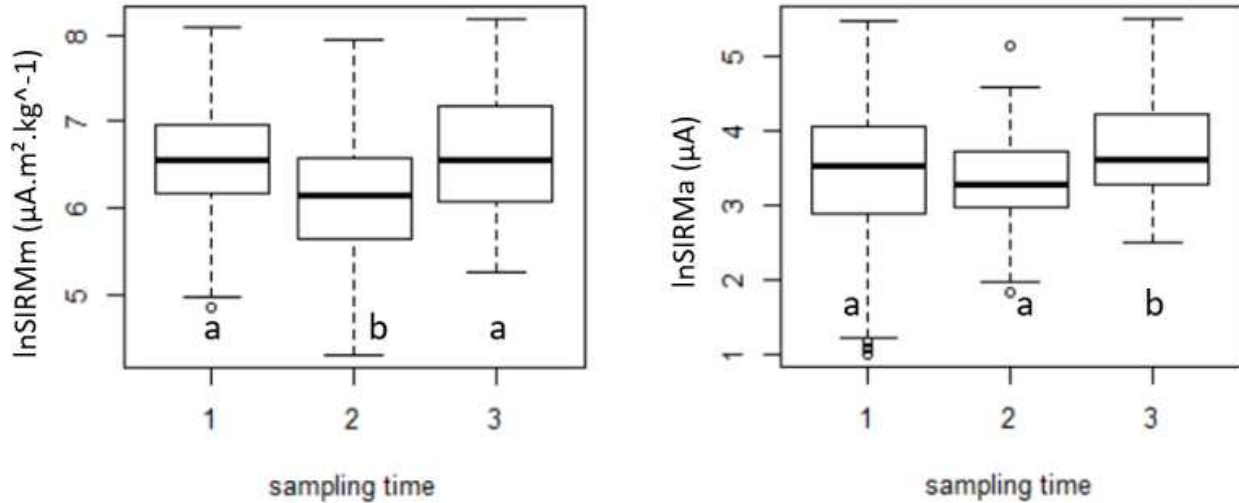
248

249 Figure 3: Total normalized ln transformed SIRM values (totalSIRM) of species in ascending order (right
 250 axis). Average SIRMa and WLAI are both shown on the left axis. Species abbreviations can be found in
 251 Appendix table 1.

252

253 3.3 Effect of sampling time – seasonal variation

254 When all species and heights are considered in the model, variation in SIRMm and SIRMa values can be
 255 found between sampling moments (Fig. 4). For SIRMm, sampling 2 was significantly different from 1 and
 256 3. For SIRMa, sampling time 3 was significantly different from the others.

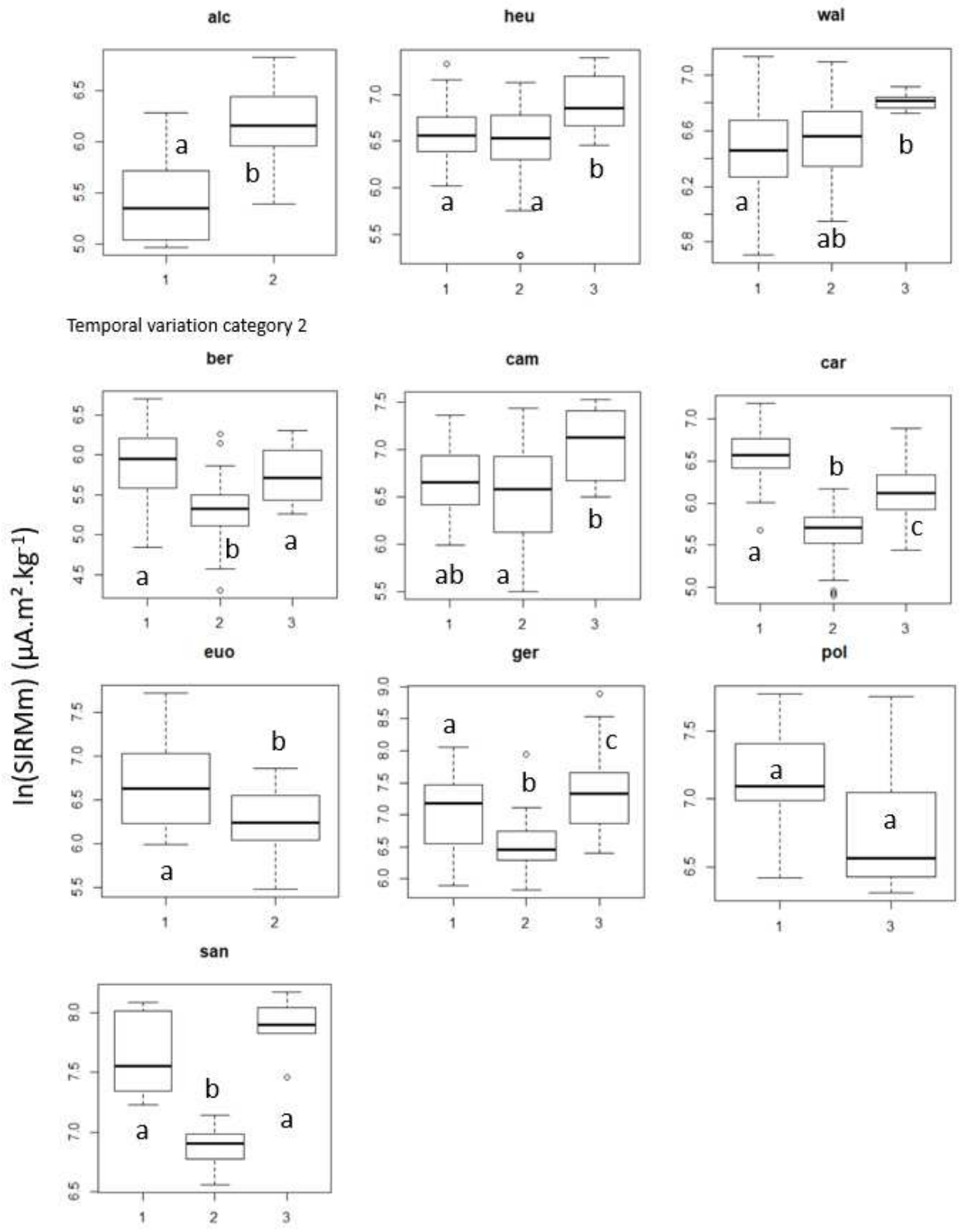


257

258 Figure 4: Boxplots of InSIRMm values at the three sampling moments (1, 2 and 3). Values with different
 259 letters (a-b) are significantly ($p < 0.05$) different.

260

261 Temporal patterns appear to be very different between species, both for SIRMm (Figure 5) and SIRMa
 262 (Figure 6). We categorized these patterns into 2 categories. For *Alchemilla mollis* (SIRMm and SIRMa),
 263 *Campanula* sp. (SIRMa), *Geranium* sp. (SIRMa), *Heuchera* sp. (SIRMm), *Polypodium vulgare* (SIRMa) and
 264 *Walsteinia ternata* (SIRMm and SIRMa), we observed a general increase of values in time, hereafter
 265 referred to as Category 1. Furthermore, *Bergenia cordifolia* (SIRMm and SIRMa), *Campanula* sp. (SIRMm),
 266 *Carex* sp. (SIRMm and SIRMa), *Euonymus fortunei* (SIRMm), *Geranium* sp. (SIRMm), *Heuchera* sp. (SIRMa),
 267 *Polypodium vulgare* (SIRMm) and *Santolina chamaecyparissus* (SIRMm and SIRMa) showed values that
 268 decreased or remained the same during the growing season, hereafter referred to as Category 2. Note
 269 that not every species could be sampled at every sampling moment. *Lonicera nitida* has been omitted from
 270 this analysis because it was only sampled the first time due to later removal of the walls that contained
 271 this species.



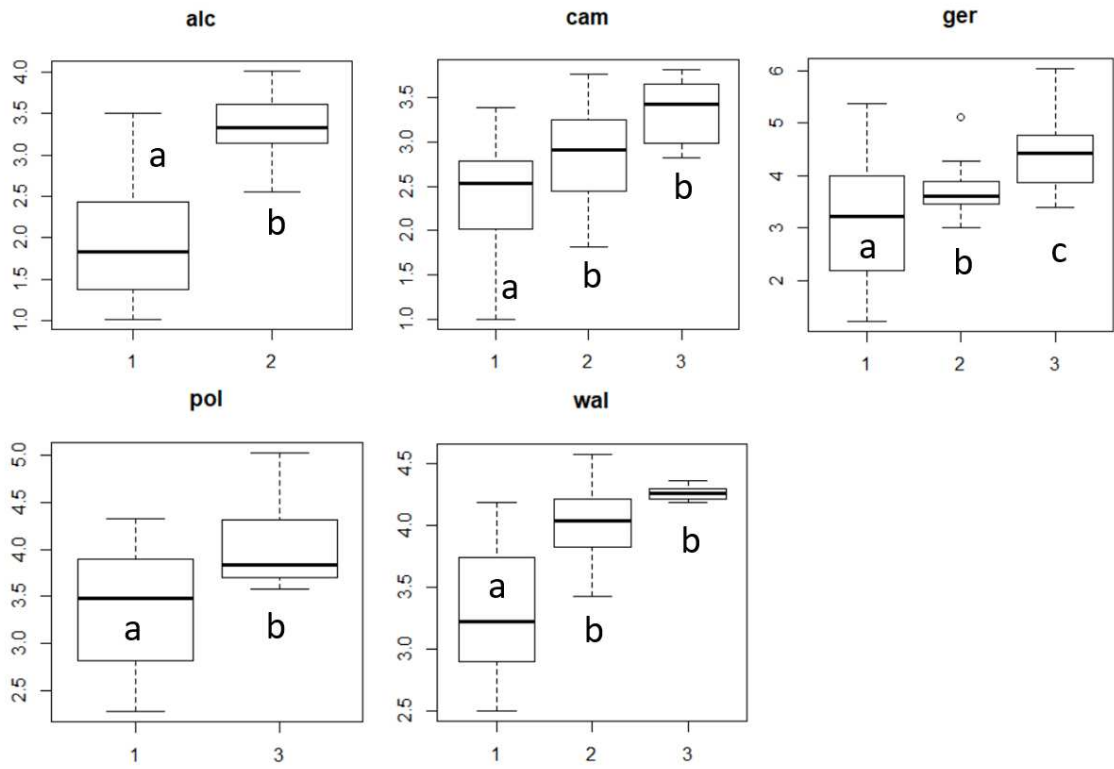
272

273

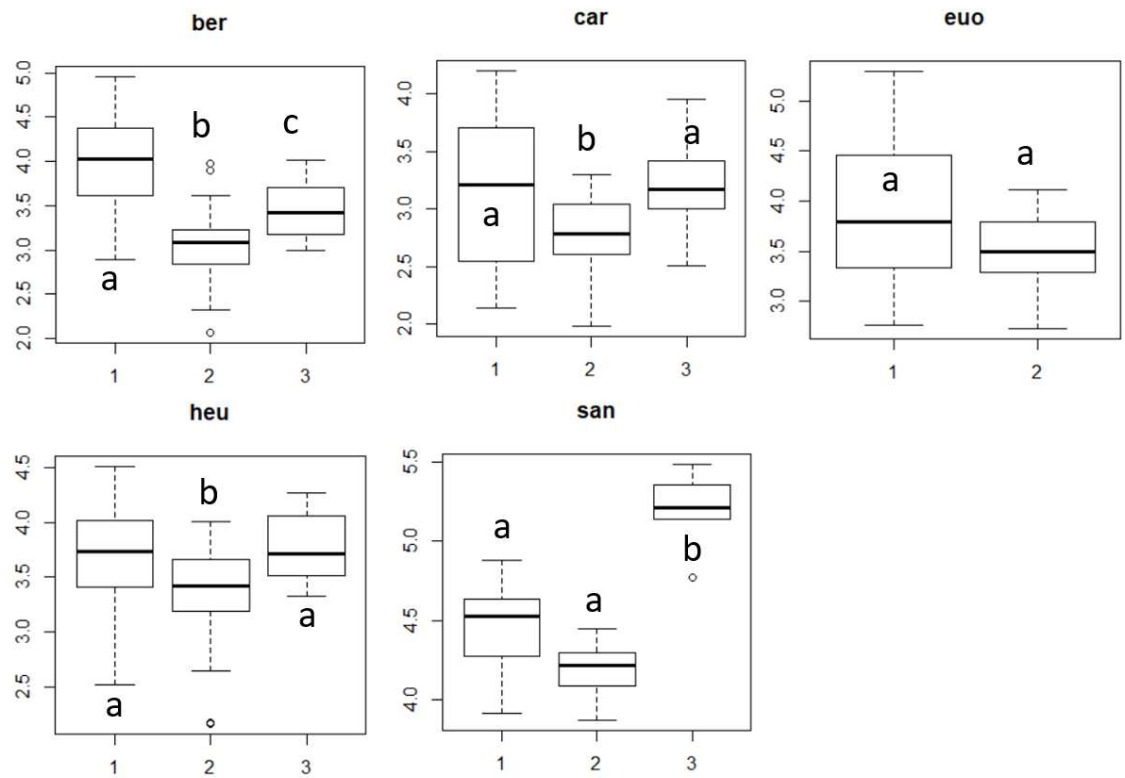
274 Figure 5: Boxplots of temporal variation of the mass normalized SIRM values (SIRM_m) for all species
275 (abbreviations are clarified in Appendix table 1) for the three sampling dates: sampling 1 (28-04-2017),
276 sampling 2 (24-08-2017), sampling 3 (20-03-2018). Species with different letters (a-c) are significantly (p <
277 0.05) different.

Temporal variation category 1

ln(SIRMa) (μ A)



Temporal variation category 2

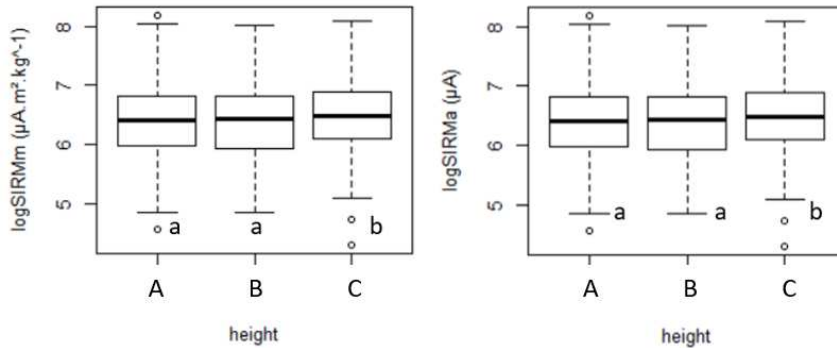


279 Figure 6: Boxplots of temporal variation of the area normalized SIRM values (SIRMa) for all species
280 (abbreviations are clarified in Appendix table 1) for the three sampling dates: sampling 1 (28-04-2017),
281 sampling 2 (24-08-2017), sampling 3 (20-03-2018). Species with different letters (a-c) are significantly ($p <$
282 0.05) different.

283

284 3.4 Influence of height

285 Vegetation was also sampled at different heights above the ground and this parameter was considered in
286 the same model as the parameters species, sampling time and wall-ID. A indicates the highest sampling
287 point (2.5 ± 0.2 m) on a LWS while C is the lowest (0.5 ± 0.2 m). Significant differences between heights A
288 and B vs. C were found (Fig. 7). For both SIRMm and SIRMa the highest values were found at the lowest
289 sampling height.



290

291 Figure 7: Boxplots of the three sampling heights (A: 2.5 ± 0.2 m), (B: 1.5 ± 0.2 m) and (C: 0.5 ± 0.2 m).

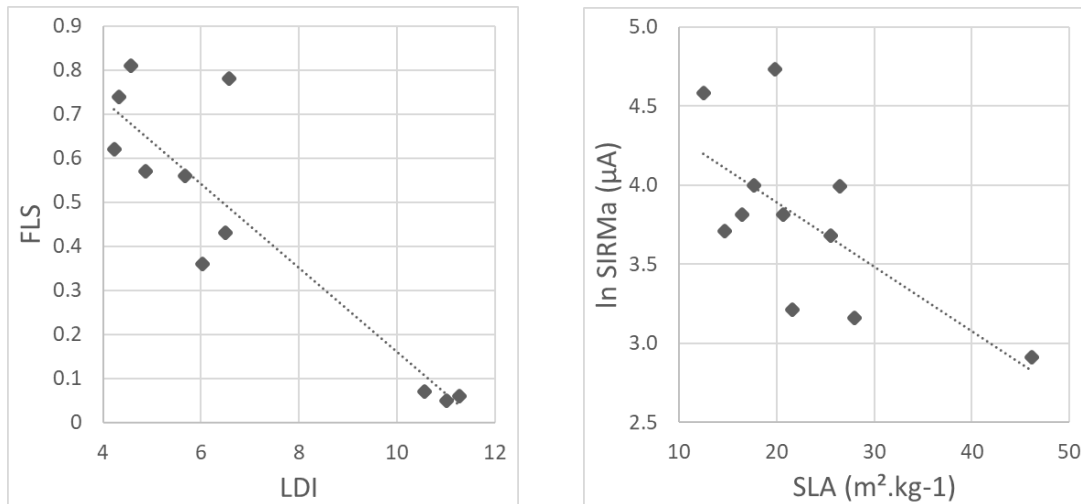
292 Left: SIRM normalized for mass (SIRMm), right: SIRM normalized for area (SIRMa). Species with different
293 letters (a-b) are significantly ($p < 0.05$) different.

294

295 3.5 Effect of morphological parameters

296 All mean values of the morphological parameters are shown in Appendix table 4. Before testing against
297 SIRM values, correlations between all morphological parameters were tested against each other. Only LDI
298 and FLS showed to be negatively correlated (Fig. 8). Furthermore, morphological parameters were
299 statistically tested against mean SIRMm and SIRMa values using a linear model. For SIRMm, no variation
300 could be explained by any of the morphological parameters. However, SIRMa showed almost interaction
301 with SLA in the linear model considering all parameters. Therefore, SLA was isolated and significantly
302 negatively contributed to the variation in SIRMa ($p < 0.05$, Fig. 8). For *Santolina chamaecyparissus*, no drop
303 contact angle could be determined due to its complex leaf shape.

304



305
306 Figure 8: Left: Correlation between leaf dissection index (LDI) and functional leaf size (FLS). FLS = -
307 $0.0953 \cdot \text{LDI} + 1.1147$. $R^2 = 0.8137$, $p < 0.05$. Right: Correlation between specific leaf area (SLA, in $\text{m}^2 \cdot \text{kg}^{-1}$)
308 and the In of the saturation isothermal remanent magnetization normalized for leaf area (ln SIRMa, in μA).
309 $\ln \text{SIRMa} = -0.0407 \cdot \text{SLA} + 4.7048$. $R^2 = 0.4455$, $p < 0.05$.

310

311 4 Discussion

312 4.1 Difference in PM accumulation between species

313 This study is the first to apply the SIRM technique to green wall plant species specifically. Magnetic
314 biomonitoring of plant leaves has been proposed as a good indicator of ambient traffic-derived PM
315 (Castañeda-Miranda et al. 2020; Chen et al. n.d.; Fusaro et al. 2021; Hofman et al. 2013; Matzka and Maher
316 1999; Winkler et al. 2022). The LWS in this common garden experiment were all exposed to the same
317 source, which allowed the researchers to make use of SIRM as a proxy for leaf deposited PM. When looking
318 at species and their PM load per leaf area (SIRMa) and per mass (SIRMm), large relative differences were
319 found (SIRMa values of 2.74 up to 417 μA). Compared to the range found by Muhammad et al. (2019) (0.7
320 to 31.6 μA) our SIRMa values are higher. We believe this is partly because of the difference in location of
321 the test site; our common garden had a more open character and was in proximity of a rail road, while the
322 common garden of Muhammad et al. (2019) was in a more secluded area, surrounded by high buildings
323 and trees and further away from a direct pollution source. We must point out that area measurement of
324 *S. chamaecyparissus* may be underestimated, due to the three dimensional shape of the leaves (unlike
325 other species that had more flattened leaves). This could result in an overestimation of SIRMa. However,
326 for SIRMm, *S. chamaecyparissus* also scored highest so it can be assumed that it is generally a good PM
327 accumulator. *L. nitida* and *Geranium* sp. also scored high for both methods. In general, we suspect that
328 relative differences between species are due to differences in morphologies.

329

330 4.2 Influence of morphological parameters

331 In many studies, differences in PM accumulation capacity between species are believed to be caused by
332 the species-specific morphological characteristics (Litschke & Kuttler 2008; Perini et al. 2017; Weerakkody
333 et al. 2017; Muhammad et al. 2019). In this study, seven morphological parameters were assessed

334 (Appendix table 4). A significant negative correlation was found between SIRMa and SLA (Fig. 8, right). This
335 means that leaves with a larger two-dimensional leaf area compared to their dry mass accumulate less PM
336 than e.g. smaller, more rigid leaves. On the left of Figure 8 (right) there are the more 'fleshy' leaves and
337 on the right we see the thinner leaves. This is in accordance with Muhammad et al. (2019, 2020), who
338 suggested that SLA (together with LDI) is a good predictor of PM accumulation and immobilisation by
339 vegetation, as a proxy for the complex interactions of various leaf morphological characteristics. This is
340 valuable for urban managers in terms of optimizing LWS design in terms of urban air quality; smaller, rigid
341 leaves are more desirable.

342 For the other morphological parameters, no correlation with SIRMm or SIRMa values was found. This is in
343 accordance with the findings of Chen et al. (2016), who also found differences in PM capture between
344 species, without demonstrable species-specific criteria. Paull et al. (2019) also found no evidence for the
345 influence of leaf morphology on PM accumulation. It is possible that the total amount of environmental
346 PM was not well enough represented by its magnetic fraction, which usually represents the anthropogenic
347 metallic fraction of PM, in urban contexts often dominated by vehicular traffic (Winkler et al. 2021) in
348 order to determine differences caused by plant morphology. Other literature suggests that grass-like
349 species (like *Carex* sp.) often do not show strong PM accumulation due to their soft or bendable structure
350 that causes less turbulence than over leaves of other vegetation species (Leonard et al. 2016; Weerakkody
351 et al. 2018a). This was also found in our study; *Carex* sp. was situated at the lower end of the net PM
352 accumulation capacity distribution. Moreover, Weerakkody (2018a) found that palmately lobed leaves
353 were the best PM accumulators, regardless of size. In our study however, LDI and FLS, which are measures
354 of leaf shape, had no significant effect on PM capture efficiency. However, they are both correlated with
355 each other (Fig. 8). This is in accordance with Weerakkody et al. (2018a) who also found LDI to be an
356 insignificant parameter. In some literature a rigidity factor is suggested (Koch et al. 2020) and air flow and
357 turbulence may be more important than plant morphology itself (Chen et al. 2016; Koch et al. 2019).

358 Therefore, we suggest wind tunnel experiments where aerodynamic properties (i.e. leaf boundary layer,
359 vegetation porosity, turbulent air flow, etc.) can be monitored and where an aerodynamic indicator can
360 be determined under controlled conditions.

361 Similar to the findings of Perini et al. (2017), Weerakkody et al. (2018b) and Paull et al. (2019), we found
362 no interaction between amount and length of trichomes and PM accumulation. Other researches
363 contradict this (Beckett et al. 2000; Kardel et al. 2012; Saebo et al. 2012; Leonard et al. 2016; Weerakkody
364 et al. 2018a; Muhammad et al. 2019), stating that hairy leaves can capture more PM because the hairs
365 inhibit resuspension by wind or rain, and they increase the surface area available for capture. On the other
366 hand, a high abundance of trichomes makes a leaf hydrophobic, altering leaf wettability, which can result
367 in an opposite effect (Muhammad et al. 2019). We assume this is the case for *A. mollis*. Furthermore, there
368 is also a wide variation of trichome size, length and texture (Weerakkody et al. 2018b) which can result in
369 very different effects. Some of the plant species examined here can be compared with plant species from
370 other manuscripts. In this study *Geranium* sp. has moderate to high PM capture, comparable to *G.*
371 *macrorrhizum* in the study by Weerakkody et al. (2018a). *B. cordifolia* scored low to medium in this study,
372 which was also the case according to Weerakkody et al. (2018a), who attributed this to the smooth surface
373 of the species.

374 Drop contact angle is often seen as a measure for the hydrophobicity or wettability of the epicuticular wax
375 layer, but was in this study also inconclusive with regard to PM accumulation. This is in accordance with
376 the research by Saebo et al. (2012), Kardel et al. (2012) and Leonard et al. (2016). On the other hand,
377 Muhammad et al. (2019) found lower PM accumulation on leaves that were more hydrophobic. We
378 suspect that general microtopography is more important than the presence of hair or wax layer properties
379 such as ridges and grooves. This is also suggested by Kardel et al. (2012).

380

381 4.3 Seasonal variation

382 The mixed model showed significant differences in PM load on the LWS over the growing season. However,
383 the course between SIRMm and SIRMa is different (Fig. 4), making it necessary to analyze each species
384 separately. The graphs in Figures 10 and 11 show the seasonal variation of individual species. These were
385 divided into two categories. The first category includes all species that have the most obvious result for
386 both PM measuring methods, i.e. an increase over time. This is in accordance to the findings of Wang et
387 al. (2013), among others, who used the gravimetric method for tree species and found that mature leaves
388 had a higher PM load than younger leaves. Our species, evergreen or not, had not changed their leaves
389 yet at the third sampling in the next Spring, which explains the high PM load. *A. mollis* leaves were not yet
390 present at the time of the third sampling as they also emerge later in the season.

391 The second category consists of species whose PM load decreases or remains the same during the growing
392 season and after winter, while new leaves had not yet emerged during the third sampling. For these
393 species, we believe that the decrease or stagnation in PM load during the growing season is mainly due to
394 PM dilution due to rapid leaf expansion. In other words, leaves expand faster than PM is deposited during
395 the growing season (sampling 1 to 2). Because the green walls have controlled watering systems with
396 added nutrients and are therefore in fairly ideal conditions, rapid growth is likely. Hofman et al. (2014)
397 found similar results for *Platanus* leaves when only the leaf encapsulated fraction of PM was considered
398 (when wash-off was excluded), further supporting our hypothesis. Subsequently, when the leaves reach
399 maturation in late summer, PM accumulation per surface or mass will increase again until senescence. An
400 additional explanation for this phenomenon could be the reduction of pollution input at the sampling site
401 during the growing season, similar to the observations by Castanheiro et al. (2020). They observed an
402 increase in PM load during the first six sampling weeks for strawberry, after which PM levels decreased
403 again. Furthermore, resuspension by rainfall or wind can differ greatly between species due to
404 micromorphology and plant porosity (Currie & Bass 2008; Przybysz et al. 2014). In contrast, Ottel  et al.

405 (2010) and Perini et al. (2017) found that seasonal variation did not affect PM accumulation. To further
406 examine seasonal variation and the influence of meteorological conditions, laboratory experiments with
407 controlled precipitation are recommended. It should also be noted that PM assessment techniques differ
408 between our study and some of the literature we refer to (SIRM versus gravimetric or electron microscopic
409 analyses), which makes direct comparison difficult, but general trends should be the same.

410 We believe that the different temporal variation categories are also influenced by leaf age uncertainty; *E.*
411 *fortunei*, *L. nitida* and *S. chamaecyparissus* are evergreens, while the other species change leaves, but also
412 in different time frames. This makes it very difficult to estimate the actual age of the leaf. In order to
413 counter this, although very labor-intensive, labeling leaves would be a good option.

414

415 4.4 Effect of WLAI

416 Since SIRM_a is a PM measure normalized for leaf area, it can be derived from this value how much the PM
417 collection capacity is for a given amount of leaf material. Obviously, WLAI changes throughout the season,
418 but given the large amount of leaves needed and not to visually damage the systems, samples for leaf area
419 determination were only taken during the pruning season. Therefore, each species has only one value for
420 WLAI, which is at least a good representation of the differences between species, and consequently also
421 only one value for totalSIRM. When SIRM_a is multiplied with WLAI, the order of species from low to high
422 PM capture capacity changes slightly, but generally remains the same; *S. chamaecyparissus*, *Geranium* sp.
423 and *L. nitida* again perform the best, together with *W. ternata*. In general, a higher WLAI is believed to be
424 better in terms of PM capture (Weerakkody et al. 2017). However, it should be noted that WLAI only
425 expresses the total amount of leaf area per wall area and not the three-dimensional plant configuration.

426 4.5 Vegetation height

427 In general, biomagnetic monitoring has been proven useful for assessing the three-dimensional spatial
428 distribution of particulates (Mitchell & Maher 2009; Kardel et al. 2011; Hofman et al. 2013). Hofman et al.
429 (2013) found that SIRM values decrease exponentially with tree leaf sampling height and tree crown
430 height, respectively. SIRM is a grainsize dependent magnetic parameter; thus, the use of SIRM as a proxy
431 for the concentration of airborne PM must be done under the assumption that particle size is constant.
432 This could not be the case for different sampling heights, because heavier particles gravitationally stay
433 closer to the ground than finer particles and thus particle size is not equally distributed over the walls
434 vertically. Moreover, the finest ultrafine particles, that are superparamagnetic at room temperature, do
435 not contribute to SIRM. So, for determining the magnetic properties according to the grainsize, the
436 combined use of magnetic susceptibility, hysteresis loops and electron microscopy techniques should be
437 applied.

438 The highest values for both SIRM_m and SIRM_a were found at the lowest sampling height, i.e. 0.2 – 0.5 m
439 above the ground (Fig. 7). This is in accordance with the majority of literature on the spatial difference in
440 SIRM values. This could mean that, when traffic is the main pollution source, it is most effective when
441 green walls are applied from ground level and upwards for pedestrian health then when they are only
442 applied from a certain building wall height. However, because SIRM is dependent on particle composition
443 and size and heavier particles tend to stay closer to the ground, there is still some uncertainty regarding
444 height differences.

445

446 4.6 Consequences for human health

447 The bioaccumulation of PM in this study was solely defined with SIRM. This technique has proven to be
448 very useful when it comes to biomonitoring analyses and big data collection, in the lab of the researchers

449 and many others (Hofman et al. 2017). However, it has to be noted that this method only works for health
450 assessment when harmful PM is well represented by its magnetic fraction (Winkler et al. 2021). This is not
451 necessarily the case in this study, as ultrafine particles probably settle at the highest heights, but do not
452 contribute to SIRM, and therefore no suggestions can be given health-wise. In exceptional cases there can
453 even be a negative correlation between SIRM and airborne PM concentrations (Petrovský et al. 2020) .
454 However, because our study was a common garden experiment with the same PM sources and
455 meteorological conditions, we assume this very unlikely. The fact that SIRM does not take into account the
456 smallest magnetic PM fraction (magnetite < 35nm), which also has the most implications for health, also
457 deserves more attention.

458

459 5 Conclusion

460 In this study, 11 commonly used living wall system (LWS) plant species were assessed in a common garden
461 experiment via SIRM (*Saturation isothermal remanent magnetization*, both normalized for leaf area and
462 mass) in terms of relative particulate matter (PM) accumulation and its change over time and in height.
463 Large differences in total SIRM values between species were found. *S. chamaecyparissus*, *Geranium sp.*, *L.*
464 *nitida* and *W. ternata* were the best PM capturers. In general, we can conclude that green wall plant
465 species are definitely able to capture PM out of the environment. However, careful species selection and
466 implementation is important. This study shows how complex interactions can be between an engineered
467 vegetation system and its environment and demonstrates the need for optimal plant composition and
468 system design. Specific leaf area (SLA) showed a negative correlation with SIRM normalized for leaf area
469 (SIRMa). This suggests that SLA is a good representative for the leaf morphological complex. Hereby it is
470 interesting for LWS designers, professionally or self-builders, to select plant species based solely on their
471 fleshy or thin appearance, in order to have an idea of their relative PM accumulation capacity, without the

472 need for PM analysis on the leaves, which is much more time consuming and expensive. Furthermore,
473 species that perform poorly in PM accumulation per unit area cannot make up for this by simply making
474 lots of leaves. It is important to include wall leaf area index (WLAI) because the species that perform best
475 taking the WLAI into account are not necessarily the species that score highest in terms of PM
476 accumulation (SIRM).

477 For future research we suggest additional laboratory experiments under controlled circumstances: correct
478 leaf age assessment by tagging, leaf expansion, senescence, monitored PM deposition, resuspension and
479 controlled precipitation and irrigation. These 'ideal' conditions could be a proxy for making estimates for
480 outdoor situations, which can then provide a comparison with this experiment. Furthermore it would be
481 useful to assess further magnetic parameters, e.g. sensitive to ultrafine particles or grain size independent
482 for the total concentration. Taking foliage permeability and porosity into account would also greatly
483 contribute to a better understanding of how air flows through vegetation and its three-dimensional
484 structure. Nevertheless, field experiments examining the systems under their real conditions remain as
485 important.

486

487 6 Acknowledgements

488 This work was supported by the FWO-SBO project 'EcoCities: Green roofs and walls as a source for
489 ecosystem services in future cities' (S002818N).

490 The authors would like to show special thanks to the EUREC-AIR lab-assistant Elisabeth Schuermans for
491 help with laboratory analyses, organization and general support.

492 7 Bibliography

493 EEA. (2017a). *Environmental indicator report 2017: Outdoor air quality in urban areas*. European
494 Environment Agency, Copenhagen.

495 EEA. (2017b). *Environmental indicator report 2017: Air pollutant emissions*. European Environment
496 Agency, Copenhagen.

497

498 Abhijith, K. V., Prashant Kumar, John Gallagher, Aonghus McNabola, Richard Baldauf, Francesco Pilla,
499 Brian Broderick, Silvana Di Sabatino, and Beatrice Pulvirenti. 2017. 'Air Pollution Abatement
500 Performances of Green Infrastructure in Open Road and Built-up Street Canyon Environments – A
501 Review'. *Atmospheric Environment* 162:71–86. doi: 10.1016/j.atmosenv.2017.05.014.

502 Beckett, K. P., P. H. Freer-Smith, and G. Taylor. 1998. 'Urban Woodlands: Their Role in Reducing the
503 Effects of Particulate Pollution'. *Environmental Pollution* 99(3):347–60. doi: 10.1016/S0269-
504 7491(98)00016-5.

505 Beckett, K. Paul, P. H. Freer-Smith, and Gail Taylor. 2000. 'Particulate Pollution Capture by Urban Trees:
506 Effect of Species and Windspeed'. *Global Change Biology* 6(8):995–1003. doi: 10.1046/j.1365-
507 2486.2000.00376.x.

508 Brunekreef, Bert. 1997. 'Air Pollution and Life Expectancy: Is There a Relation?' *Occupational and
509 Environmental Medicine* 54(11):781–84. doi: 10.1136/oem.54.11.781.

510 Castañeda-Miranda, Ana G., Marcos A.E. Chaparro, Adolfo Pacheco-Castro, Mauro A.E. Chaparro, and
511 Harald N. Böhnel. 2020. 'Magnetic Biomonitoring of Atmospheric Dust Using Tree Leaves of Ficus
512 Benjamina in Querétaro (México)'. *Environmental Monitoring and Assessment* 192(6). doi:
513 10.1007/s10661-020-8238-x.

514 Castanheiro, Ana, Jelle Hofman, Gert Nuyts, Steven Joosen, Simo Spassov, Ronny Blust, Silvia Lenaerts,
515 Karolien De Wael, and Roeland Samson. 2020. 'Leaf Accumulation of Atmospheric Dust:
516 Biomagnetic, Morphological and Elemental Evaluation Using SEM, ED-XRF and HR-ICP-MS'.
517 *Atmospheric Environment* 221(October 2019):117082. doi: 10.1016/j.atmosenv.2019.117082.

518 Castanheiro, Ana, Roeland Samson, and Karolien De Wael. 2016. 'Magnetic- and Particle-Based
519 Techniques to Investigate Metal Deposition on Urban Green'. *Science of the Total Environment*
520 571:594–602. doi: 10.1016/j.scitotenv.2016.07.026.

521 Chen, Hong, &. Dun-Sheng Xia, Bo Wang, Hui Liu, and Xiaoyi Ma. n.d. 'Pollution Monitoring Using the
522 Leaf-Deposited Particulates and Magnetism of the Leaves of 23 Plant Species in a Semi-Arid City,
523 Northwest China'. doi: 10.1007/s11356-021-16686-1/Published.

524 Chen, Lixin, Chenming Liu, Rui Zou, Mao Yang, and Zhiqiang Zhang. 2016. 'Experimental Examination of
525 Effectiveness of Vegetation as Bio-Filter of Particulate Matters in the Urban Environment'.
526 *Environmental Pollution* 208:198–208. doi: 10.1016/j.envpol.2015.09.006.

527 Currie, Beth Anne, and Brad Bass. 2008. 'Estimates of Air Pollution Mitigation with Green Plants and
528 Green Roofs Using the UFORE Model'. *Urban Ecosystems* 11(4):409–22. doi: 10.1007/s11252-008-
529 0054-y.

530 Declercq, Ynse, Roeland Samson, Ellen Van De Vijver, Johan De Grave, Filip M. G. Tack, and Philippe De
531 Smedt. 2020. 'A Multi-Proxy Magnetic Approach for Monitoring Large-Scale Airborne Pollution
532 Impact'. *Science of the Total Environment* 743:140718. doi: 10.1016/j.scitotenv.2020.140718.

533 Van Dyck, Lieve, Hayat Bentouhami, Kyra Koch, Roeland Samson, and Joost Weyler. 2019. 'Exposure to
534 Indoor Ferromagnetic Particulate Matter Monitored by Strawberry Plants and the Occurrence of

535 Acute Respiratory Events in Adults'. *International Journal of Environmental Research and Public*
536 *Health* 16(23):1–10. doi: 10.3390/ijerph16234823.

537 Dzierzanowski, Kajetan, Robert Popek, Helena Gawrońska, Arne Saebø, and Stanislaw W. Gawroński.
538 2011. 'Deposition of Particulate Matter of Different Size Fractions on Leaf Surfaces and in Waxes of
539 Urban Forest Species'. *International Journal of Phytoremediation* 13(10):1037–46. doi:
540 10.1080/15226514.2011.552929.

541 Freer-Smith, P. H., K. P. Beckett, and Gail Taylor. 2005. 'Deposition Velocities to Sorbus Aria, Acer
542 Campestre, Populus Deltoides x Trichocarpa "Beaupré", Pinus Nigra and x Cupressocyparis Leylandii
543 for Coarse, Fine and Ultra-Fine Particles in the Urban Environment'. *Environmental Pollution*
544 133(1):157–67. doi: 10.1016/j.envpol.2004.03.031.

545 Fusaro, Lina, Elisabetta Salvatori, Aldo Winkler, Maria Agostina Frezzini, Elena De Santis, Leonardo
546 Sagnotti, Silvia Canepari, and Fausto Manes. 2021. 'Urban Trees for Biomonitoring Atmospheric
547 Particulate Matter: An Integrated Approach Combining Plant Functional Traits, Magnetic and
548 Chemical Properties'. *Ecological Indicators* 126. doi: 10.1016/j.ecolind.2021.107707.

549 Gallagher, John, Richard Baldauf, Christina H. Fuller, Prashant Kumar, Laurence W. Gill, and Aonghus
550 McNabola. 2015. 'Passive Methods for Improving Air Quality in the Built Environment: A Review of
551 Porous and Solid Barriers'. *Atmospheric Environment* 120:61–70. doi:
552 10.1016/j.atmosenv.2015.08.075.

553 Hofman, Jelle, Barbara A. Maher, Adrian R. Muxworthy, Karen Wuyts, Ana Castanheiro, and Roeland
554 Samson. 2017. 'Biomagnetic Monitoring of Atmospheric Pollution: A Review of Magnetic Signatures
555 from Biological Sensors'. *Environmental Science and Technology* 51(12):6648–64. doi:
556 10.1021/acs.est.7b00832.

557 Hofman, Jelle, Ines Stokkaer, Lies Snauwaert, and Roeland Samson. 2013. 'Spatial Distribution
558 Assessment of Particulate Matter in an Urban Street Canyon Using Biomagnetic Leaf Monitoring of
559 Tree Crown Deposited Particles.' *Environmental Pollution (Barking, Essex : 1987)* 183:123–32. doi:
560 10.1016/j.envpol.2012.09.015.

561 Hofman, Jelle, Karen Wuyts, Shari Van Wittenberghe, Melanka Brackx, and Roeland Samson. 2014. 'On
562 the Link between Biomagnetic Monitoring and Leaf-Deposited Dust Load of Urban Trees:
563 Relationships and Spatial Variability of Different Particle Size Fractions'. *Environmental Pollution*
564 192:285–94. doi: 10.1016/j.envpol.2014.05.006.

565 Hofman, Jelle, Karen Wuyts, Shari Van Wittenberghe, and Roeland Samson. 2014. 'On the Temporal
566 Variation of Leaf Magnetic Parameters: Seasonal Accumulation of Leaf-Deposited and Leaf-
567 Encapsulated Particles of a Roadside Tree Crown'. *Science of The Total Environment* 493:766–72.
568 doi: 10.1016/j.scitotenv.2014.06.074.

569 Hussain Lakho, Fida, Jarne Vergote, Hafiz Ihsan-ul-haq Khan, Veerle Depuydt, Teun Depreeuw, Stijn Van
570 Hulle, and Diederik Rousseau. 2021. 'Total Value Wall : Full Scale Demonstration of a Green Wall for
571 Grey Water Treatment and Recycling'. *Journal of Environmental Management* 298(July):113489.
572 doi: 10.1016/j.jenvman.2021.113489.

573 Janhäll, Sara. 2015. 'Review on Urban Vegetation and Particle Air Pollution - Deposition and Dispersion'.
574 *Atmospheric Environment* 105:130–37. doi: 10.1016/j.atmosenv.2015.01.052.

575 Jimoda, L. A. 2012. 'Effects of Particulate Matter on Human Health, Climate and Materials: A Review'.
576 *Working and Living Environmental Protection* 9(1):27–44.

577 Kardel, F., K. Wuyts, B. a. Maher, R. Hansard, and R. Samson. 2011. 'Leaf Saturation Isothermal
578 Remanent Magnetization (SIRM) as a Proxy for Particulate Matter Monitoring: Inter-Species

579 Differences and in-Season Variation'. *Atmospheric Environment* 45(29):5164–71. doi:
580 10.1016/j.atmosenv.2011.06.025.

581 Kardel, F., K. Wuyts, B. a. Maher, and R. Samson. 2012. 'Intra-Urban Spatial Variation of Magnetic
582 Particles: Monitoring via Leaf Saturation Isothermal Remanent Magnetisation (SIRM)'. *Atmospheric
583 Environment* 55:111–20. doi: 10.1016/j.atmosenv.2012.03.025.

584 Koch, K., R. Samson, and S. Denys. 2019. 'Aerodynamic Characterisation of Green Wall Vegetation Based
585 on Plant Morphology: An Experimental and Computational Fluid Dynamics Approach'. *Biosystems
586 Engineering* 178. doi: 10.1016/j.biosystemseng.2018.10.019.

587 Koch, Kyra, Roeland Samson, and Siegfried Denys. 2020. 'Experimental and Computational Aerodynamic
588 Characterisation of Urban Trees'. *Biosystems Engineering* 190(2019):47–57. doi:
589 10.1016/j.biosystemseng.2019.11.020.

590 Koch, Kyra, Tess Ysebaert, Siegfried Denys, and Roeland Samson. 2020. 'Urban Heat Stress Mitigation
591 Potential of Green Walls: A Review'. *Urban Forestry and Urban Greening* 55(July):126843. doi:
592 10.1016/j.ufug.2020.126843.

593 Leonard, Ryan J., Clare McArthur, and Dieter F. Hochuli. 2016. 'Particulate Matter Deposition on
594 Roadside Plants and the Importance of Leaf Trait Combinations'. *Urban Forestry and Urban
595 Greening* 20:249–53. doi: 10.1016/j.ufug.2016.09.008.

596 Litschke, Tom, and Wilhelm Kuttler. 2008. 'On the Reduction of Urban Particle Concentration by
597 Vegetation - A Review'. *Meteorologische Zeitschrift* 17(3):229–40. doi: 10.1127/0941-
598 2948/2008/0284.

599 Madre, Frédéric, Philippe Clergeau, Nathalie Machon, and Alan Vergnes. 2015. 'Building Biodiversity:
600 Vegetated Façades as Habitats for Spider and Beetle Assemblages'. *Global Ecology and*
601 *Conservation* 3:222–33. doi: 10.1016/j.gecco.2014.11.016.

602 Maher, Barbara A., Imad A. M. Ahmed, Brian Davison, Vassil Karloukovski, and Robert Clarke. 2013.
603 'Impact of Roadside Tree Lines on Indoor Concentrations of Traffic-Derived Particulate Matter'.
604 *Environmental Science and Technology* 47(23):13737–44. doi: 10.1021/es404363m.

605 Matzka, J., and B. A. Maher. 1999. 'Magnetic Biomonitoring of Roadside Tree Leaves: Identification of
606 Spatial and Temporal Variations in Vehicle-Derived Particulates'. *Atmospheric Environment*
607 33(28):4565–69. doi: 10.1016/S1352-2310(99)00229-0.

608 McLellan, T., and J. A. Endler. 1998. 'The Relative Success of Some Methods for Measuring and Describing
609 the Shape of Complex Objects'. *Systematic Biology* 47(2):264–81. doi: 10.1080/106351598260914.

610 Mitchell, R., and B. A. Maher. 2009. 'Evaluation and Application of Biomagnetic Monitoring of Traffic-
611 Derived Particulate Pollution'. *Atmospheric Environment* 43(13):2095–2103. doi:
612 10.1016/j.atmosenv.2009.01.042.

613 Muhammad, S., K. Wuyts, and R. Samson. 2019. 'Atmospheric Net Particle Accumulation on 96 Plant
614 Species with Contrasting Morphological and Anatomical Leaf Characteristics in a Common Garden
615 Experiment'. *Atmospheric Environment* 202(January 2019):328–44. doi:
616 10.1016/j.atmosenv.2019.01.015.

617 Muhammad, Samira, Karen Wuyts, Gert Nuyts, Karolien De Wael, and Roeland Samson. 2020.
618 'Characterization of Epicuticular Wax Structures on Leaves of Urban Plant Species and Its
619 Association with Leaf Wettability'. *Urban Forestry and Urban Greening* 47(December 2019):126557.
620 doi: 10.1016/j.ufug.2019.126557.

621 Nowak, David J., Daniel E. Crane, and Jack C. Stevens. 2006. 'Air Pollution Removal by Urban Trees and
622 Shrubs in the United States'. *Urban Forestry and Urban Greening* 4(3–4):115–23. doi:
623 10.1016/j.ufug.2006.01.007.

624 Ottel , Marc, Hein D. van Bohemen, and a. L. a Fraaij. 2010. 'Quantifying the Deposition of Particulate
625 Matter on Climber Vegetation on Living Walls'. *Ecological Engineering* 36(2):154–62. doi:
626 10.1016/j.ecoleng.2009.02.007.

627 Paull, Naomi J., Daniel Krix, Peter J. Irga, and Fraser R. Torpy. 2019. 'Airborne Particulate Matter
628 Accumulation on Common Green Wall Plants'. *International Journal of Phytoremediation* 0(0):1–13.
629 doi: 10.1080/15226514.2019.1696744.

630 P rez, Gabriel, L dia Rinc n, Anna Vila, Josep M. Gonz lez, and Luisa F. Cabeza. 2011. 'Green Vertical
631 Systems for Buildings as Passive Systems for Energy Savings'. *Applied Energy* 88(12):4854–59. doi:
632 10.1016/j.apenergy.2011.06.032.

633 Perini, Katia, Marc Ottel , Saverio Giulini, Adriano Magliocco, and Enrica Roccotiello. 2017.
634 'Quantification of Fine Dust Deposition on Different Plant Species in a Vertical Greening System'.
635 *Ecological Engineering* 100(January):268–76. doi: 10.1016/j.ecoleng.2016.12.032.

636 Petrovsk , Eduard, Aleř Kapiřka, Hana Grison, Bohumil Kotl k, and Hana Miturov . 2020. 'Negative
637 Correlation between Concentration of Iron Oxides and Particulate Matter in Atmospheric Dust:
638 Case Study at Industrial Site during Smoggy Period'. *Environmental Sciences Europe* 32(1). doi:
639 10.1186/s12302-020-00420-8.

640 Pope III, C. Arden, and Douglas W. Dockery. 2006. 'Health Effects of Fine Particulate Air Pollution: Lines
641 That Connect'. *Journal of the Air and Waste Management Association* 56(6):709–42. doi:
642 10.1080/10473289.2006.10464485.

643 Prodanovic, Veljko, Belinda Hatt, David McCarthy, Kefeng Zhang, and Ana Deletic. 2017. 'Green Walls for
644 Greywater Reuse: Understanding the Role of Media on Pollutant Removal'. *Ecological Engineering*
645 102:625–35. doi: 10.1016/j.ecoleng.2017.02.045.

646 Przybysz, A., A. Sæbø, H. M. Hanslin, and S. W. Gawroński. 2014. 'Accumulation of Particulate Matter and
647 Trace Elements on Vegetation as Affected by Pollution Level, Rainfall and the Passage of Time'.
648 *Science of the Total Environment* 481(1):360–69. doi: 10.1016/j.scitotenv.2014.02.072.

649 Pugh, Thomas a M., a Robert Mackenzie, J. Duncan Whyatt, and C. Nicholas Hewitt. 2012. 'Effectiveness
650 of Green Infrastructure for Improvement of Air Quality in Urban Street Canyons.' *Environmental*
651 *Science & Technology* 46(14):7692–99. doi: 10.1021/es300826w.

652 Rai, Prabhat Kumar. 2016. 'Impacts of Particulate Matter Pollution on Plants: Implications for
653 Environmental Biomonitoring'. *Ecotoxicology and Environmental Safety* 129:120–36. doi:
654 10.1016/j.ecoenv.2016.03.012.

655 Sæbø, A., R. Popek, B. Nawrot, H. M. Hanslin, H. Gawronska, and S. W. Gawronski. 2012. 'Plant Species
656 Differences in Particulate Matter Accumulation on Leaf Surfaces'. *Science of the Total Environment*
657 427–428:347–54. doi: 10.1016/j.scitotenv.2012.03.084.

658 Shao, Yiming, Jiaqiang Li, Zhiwei Zhou, Fan Zhang, and Yuanlong Cui. 2021. 'The Impact of Indoor Living
659 Wall System on Air Quality: A Comparative Monitoring Test in Building Corridors'. *Sustainability*
660 *(Switzerland)* 13(14). doi: 10.3390/su13147884.

661 Solomon, Paul A., Maria Costantini, Thomas J. Grahame, Miriam E. Gerlofs-Nijland, Flemming R. Cassee,
662 Armistead G. Russell, Jeffrey R. Brook, Philip K. Hopke, George Hidy, Robert F. Phalen, Paulo Saldiva,
663 Stefanie Ebel Sarnat, John R. Balmes, Ira B. Tager, Halûk Özkaynak, Sverre Vedal, Susan S. G.

664 Wierman, and Daniel L. Costa. 2012. *Air Pollution and Health: Bridging the Gap from Sources to*
665 *Health Outcomes: Conference Summary*. Vol. 5.

666 Stalder, Aurélien F., Tobias Melchior, Michael Müller, Daniel Sage, Thierry Blu, and Michael Unser. 2010.
667 'Low-Bond Axisymmetric Drop Shape Analysis for Surface Tension and Contact Angle
668 Measurements of Sessile Drops'. *Colloids and Surfaces A: Physicochemical and Engineering Aspects*
669 364(1–3):72–81. doi: 10.1016/j.colsurfa.2010.04.040.

670 Sternberg, Troy, Heather Viles, Alan Cathersides, and Mona Edwards. 2010. 'Dust Particulate Absorption
671 by Ivy (*Hedera Helix L*) on Historic Walls in Urban Environments'. *Science of the Total Environment*
672 409(1):162–68. doi: 10.1016/j.scitotenv.2010.09.022.

673 Tallis, Matthew J., Jorge Humberto Amorim, Carlo Calfapietra, Peter Freer-Smith, Sue Grimmond, and
674 Simone Kotthaus. 2015. 'The Impacts of Green Infrastructure on Air Quality and Temperature'.
675 *Handbook on Green Infrastructure* (November):30–49. doi: 10.4337/9781783474004.00008.

676 Viecco, Margareth, Sergio Vera, Héctor Jorquera, Waldo Bustamante, Jorge Gironás, Cynnamon Dobbs,
677 and Eduardo Leiva. 2018. 'Potential of Particle Matter Dry Deposition on Green Roofs and Living
678 Walls Vegetation for Mitigating Urban Atmospheric Pollution in Semiarid Climates'. *Sustainability*
679 *(Switzerland)* 10(7). doi: 10.3390/su10072431.

680 Vos, Peter E. J., Bino Maiheu, Jean Vankerkom, and Stijn Janssen. 2012. 'Improving Local Air Quality in
681 Cities: To Tree or Not to Tree?' *Environmental Pollution* 183:113–22. doi:
682 10.1016/j.envpol.2012.10.021.

683 Wang, Huixia, Hui Shi, Yangyang Li, Ya Yu, and Jun Zhang. 2013. 'Seasonal Variations in Leaf Capturing of
684 Particulate Matter, Surface Wettability and Micromorphology in Urban Tree Species'. *Frontiers of*
685 *Environmental Science and Engineering* 7(4):579–88. doi: 10.1007/s11783-013-0524-1.

686 Weber, Frauke, Ingo Kowarik, and Ina Säumel. 2014. 'Herbaceous Plants as Filters: Immobilization of
687 Particulates along Urban Street Corridors'. *Environmental Pollution* 186:234–40. doi:
688 10.1016/j.envpol.2013.12.011.

689 Weerakkody, Udeshika, John W. Dover, Paul Mitchell, and Kevin Reiling. 2017. 'Particulate Matter
690 Pollution Capture by Leaves of Seventeen Living Wall Species with Special Reference to Rail-Traffic
691 at a Metropolitan Station'. *Urban Forestry and Urban Greening* 27(July):173–86. doi:
692 10.1016/j.ufug.2017.07.005.

693 Weerakkody, Udeshika, John W. Dover, Paul Mitchell, and Kevin Reiling. 2018a. 'Evaluating the Impact of
694 Individual Leaf Traits on Atmospheric Particulate Matter Accumulation Using Natural and Synthetic
695 Leaves'. *Urban Forestry & Urban Greening* 30(January):98–107. doi: 10.1016/j.ufug.2018.01.001.

696 Weerakkody, Udeshika, John W. Dover, Paul Mitchell, and Kevin Reiling. 2018b. 'Quantification of the
697 Traffic-Generated Particulate Matter Capture by Plant Species in a Living Wall and Evaluation of the
698 Important Leaf Characteristics'. *Science of the Total Environment* 635:1012–24. doi:
699 10.1016/j.scitotenv.2018.04.106.

700 Weerakkody, Udeshika, John W. Dover, Paul Mitchell, and Kevin Reiling. 2018. 'The Impact of Rainfall in
701 Remobilising Particulate Matter Accumulated on Leaves of Four Evergreen Species Grown on a
702 Green Screen and a Living Wall'. *Urban Forestry & Urban Greening* 35:21–31. doi:
703 10.1016/j.ufug.2018.07.018.

704 White, Emma V., and Birgitta Gatersleben. 2011. 'Greenery on Residential Buildings: Does It Affect
705 Preferences and Perceptions of Beauty?' *Journal of Environmental Psychology* 31(1):89–98. doi:
706 10.1016/j.jenvp.2010.11.002.

707 Winkler, Aldo, Antonio Amoroso, Alessandro Di Giosa, and Giada Marchegiani. 2021. 'The Effect of Covid-
708 19 Lockdown on Airborne Particulate Matter in Rome, Italy: A Magnetic Point of View'.
709 *Environmental Pollution* 291. doi: 10.1016/j.envpol.2021.118191.

710 Winkler, Aldo, Tania Contardo, Virginia Lapenta, Antonio Sgamellotti, and Stefano Loppi. 2022. 'Assessing
711 the Impact of Vehicular Particulate Matter on Cultural Heritage by Magnetic Biomonitoring at Villa
712 Farnesina in Rome, Italy'. *Science of the Total Environment* 823. doi:
713 10.1016/j.scitotenv.2022.153729.

714 Wong, Nyuk Hien, Alex Yong Kwang Tan, Yu Chen, Kannagi Sekar, Puay Yok Tan, Derek Chan, Kelly
715 Chiang, and Ngian Chung Wong. 2010. 'Thermal Evaluation of Vertical Greenery Systems for
716 Building Walls'. *Building and Environment* 45(3):663–72. doi: 10.1016/j.buildenv.2009.08.005.

717 van de Wouw, P. M. F., E. J. M. Ros, and H. J. H. Brouwers. 2017. 'Precipitation Collection and
718 Evapo(Transpi)Ration of Living Wall Systems: A Comparative Study between a Panel System and a
719 Planter Box System'. *Building and Environment* 126(July):221–37. doi:
720 10.1016/j.buildenv.2017.10.002.

721 Ysebaert, Tess, Kyra Koch, Roeland Samson, and Siegfried Denys. 2021. 'Green Walls for Mitigating Urban
722 Particulate Matter Pollution—A Review'. *Urban Forestry and Urban Greening* 59(November
723 2020):127014. doi: 10.1016/j.ufug.2021.127014.

724

The influence of plant species, leaf morphology, height and season on PM capture efficiency in living wall systems

Appendix

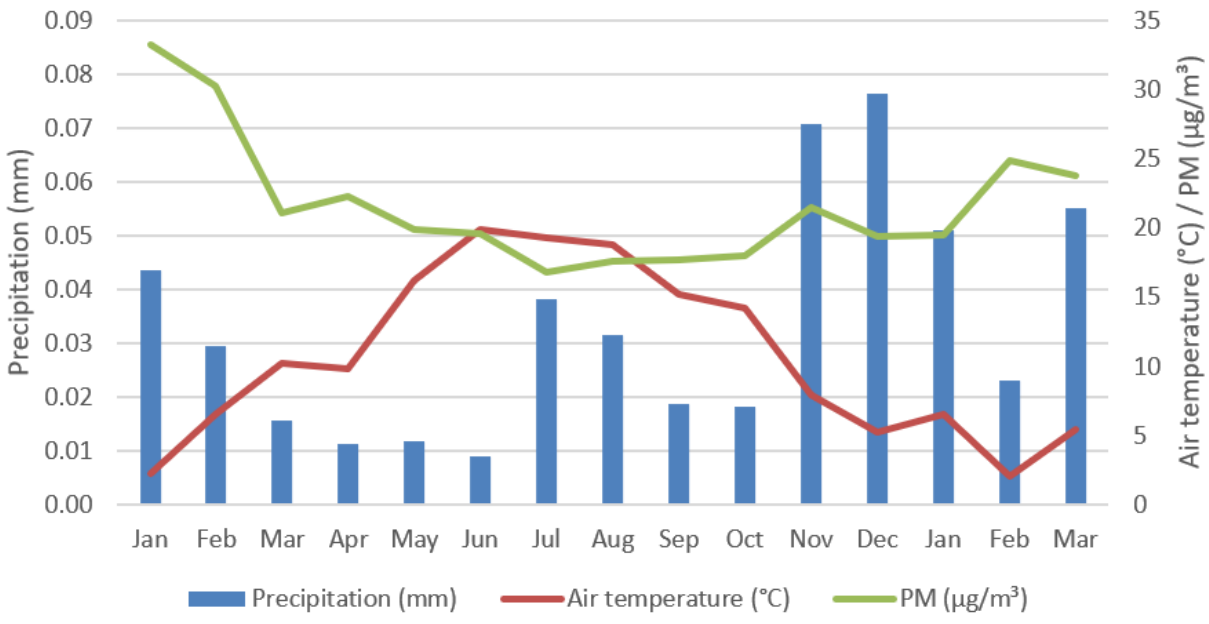
Figures



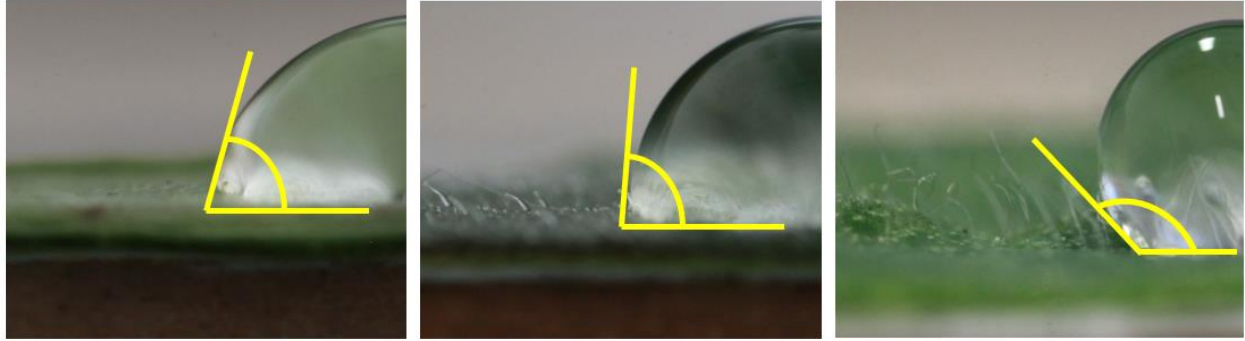
Appendix Figure 1: Location of the Testing Center for Floriculture (Proefcentrum voor Sierteelt) in proximity of Ghent city and the Port of Ghent (Gent Zeehaven) in the North. Inset: Red arrow indicates the nearest road; blue arrow indicates the rail road. (Source: Google Maps)



Appendix Figure 2: Several individual test walls on the facility at PCS, Destelbergen. Wall X was placed later, and therefore not tested.



Appendix Figure 3: Average monthly air temperature (red line), average monthly PM concentration (green line) and monthly precipitation (blue bars) from 1/01/2017 until 20/03/2018 (station M701, Tolhuiskaai, Gent and station 44R710) (source: Flanders Environmental Agency (VMM)).



Appendix Figure 4: **drop contact angle**: different angles are shown in the pictures. Hairiness: from left to right; no visible hairs (class 0), short or few visible hairs (class 1) and many or long visible hairs (class 2) as viewed through the macro lens.

Tables

Table 1: Overview of all investigated plant species, their leaf shape and the abbreviations used in the text are mentioned between brackets. Photos are not actual size, nor relative size to each other.












<i>Alchemilla mollis</i> (alc)	<i>Bergenia cordifolia</i> (ber)	<i>Campanula sp.</i> (cam)	<i>Carex sp.</i> (car)
			
<i>Euonymus fortunei</i> (euo)	<i>Geranium sp.</i> (ger)	<i>Heuchera sp.</i> (heu)	<i>Lonicera nitida</i> (lon)
			
<i>Polypodium vulgare</i> (pol)	<i>Santolina chamaecyparissus</i> (san)	<i>Waldsteinia ternata</i> (wal)	
			

Table 2: Plant species that were sampled on the different living wall systems throughout the experiment. Numbers indicate wall-ID. Species that were sampled at all three sampling dates at a certain wall are indicated with a '*'.

Species	28 April 2017	24 August 2017	20 March 2018
<i>A. mollis</i>	8	8, 11, 13	
<i>B. cordifolia</i>	1, 2, 3, 4, 6*, 8*, 11, 13	4, 6*, 8*, 11, 13	6*, 8*, 13
<i>Campanula sp.</i>	2, 5, 6*, 12,	5, 6*, 12	6*
<i>Carex sp.</i>	7*, 9*, 12, 13*	7*, 8, 9*, 12, 13*	7*, 8, 9*, 13*
<i>E. fortunei</i>	2, 3, 4, 5	5	
<i>Geranium sp.</i>	1, 7*, 8*, 12, 13	7*, 8*, 12, 13,	7*, 8*
<i>Heuchera sp.</i>	3, 4, 6, 9, 11, 12	4, 6, 9, 11, 12	6, 9
<i>L. nitida</i>	1, 11		
<i>P. vulgare</i>	6, 9		6
<i>S. chamaecyparissus</i>	7*	7*	7*
<i>W. ternate</i>	2, 3, 4, 5, 6 *	4, 5, 6*	6*

Table 3: Average wind directions per month prior to and during the sampling period. N = north, E = east, S = south, W = west (station 44R701, Baudelohof, Gent (source: Flanders Environmental Agency (VMM))).

Month	2017												2018		
	Jan	Feb	Mar	Apr	May	Jun	Jul	Aug	Sep	Oct	Nov	Dec	Jan	Feb	Mar
Wind direction	S	S	S	WSW	S	S	SW	SSW	SSW	SW	WSW	SW	SSW	SE	S

Table 4: Average morphological leaf variables +/- standard deviation for all species. DCA = drop contact angle (ad = adaxial, ab = abaxial)(degrees), SLA = specific leaf area ($m^2 \cdot kg^{-1}$), LDI = leaf dissection index (dimensionless), FLS = functional leaf size (dimensionless), hairiness categories: no visible hairs (0), short hairs (1) and long hairs (2). NA = not applicable.

Species	WLAI	DCA (ad)	DCA (ab)	SLA	LDI	FLS	Hairiness
<i>A. mollis</i>	2.37	149 (\pm 0.12)	146 (\pm 1.16)	21.63 (\pm 6.58)	5.68 (\pm 0.33)	0.56 (\pm 0.11)	2
<i>B. cordifolia</i>	2.32	96 (\pm 1.21)	56 (\pm 0.75)	14.70 (\pm 6.44)	4.32 (\pm 0.12)	0.74 (\pm 0.06)	0
<i>Campanula sp.</i>	5.41	77 (\pm 0.59)	76 (\pm 1.90)	46.11 (\pm 11.90)	4.87 (\pm 0.20)	0.57 (\pm 0.06)	1
<i>Carex sp.</i>	1.61	70 (\pm 3.06)	107 (\pm 1.52)	27.96 (\pm 4.43)	10.56 (\pm 0.92)	0.07 (\pm 0.01)	1
<i>E. fortunei</i>	2.66	76 (\pm 0.64)	92 (\pm 0.42)	17.71 (\pm 0.71)	4.57 (\pm 0.28)	0.81 (\pm 0.05)	0
<i>Geranium sp.</i>	8.19	93 (\pm 1.10)	105 (\pm 0.80)	26.50 (\pm 6.41)	6.04 (\pm 1.04)	0.36 (\pm 0.17)	2
<i>Heuchera sp.</i>	6.60	98 (\pm 0.94)	120 (\pm 0.74)	25.51 (\pm 5.04)	6.50 (\pm 0.51)	0.43 (\pm 0.09)	2
<i>L. nitida</i>	28.94	103 (\pm 1.52)	86 (\pm 1.40)	12.49 (\pm 0.43)	4.23 (\pm 0.33)	0.62 (\pm 0.05)	0
<i>P. vulgare</i>	2.61	98 (\pm 1.34)	99 (\pm 1.15)	16.49 (\pm 4.78)	11.02 (\pm 4.03)	0.05 (\pm 0.03)	0
<i>S. chamaecyparissus</i>	24.04	NA	NA	19.79 (\pm 2.78)	11.28 (\pm 2.09)	0.06 (\pm 0.03)	2
<i>W. ternata</i>	41.54	112 (\pm 2.51)	92 (\pm 0.88)	20.66 (\pm 6.20)	6.57 (\pm 0.39)	0.78 (\pm 0.08)	2